Synthesis of double ammonium/calcium pyrophosphate monohydrate $Ca(NH_4)_2P_2O_7 \cdot H_2O$ as the precursor of biocompatible phases of calcium phosphate ceramics*

T. V. Safronova,[a,b]★ A. S. Kiselev,[a] T. B. Shatalova,[a,b] Ya. Yu. Filippov,[b,c] and O. T. Gavlina[a]

[a]*Department of Chemistry, M. V. Lomonosov Moscow State University, Building 3, 1 Leninskie Gory, 119991 Moscow, Russian Federation. Fax: +7 (495) 932 8846. E-mail: t3470641@yandex.ru*
[b]*Department of Materials Science, M. V. Lomonosov Moscow State University, Building 73, 1 Leninskie Gory, 119991 Moscow, Russian Federation*
[c]*Institute of Mechanics, M. V. Lomonosov Moscow State University, 1 Michurinskii prosp., 119192 Moscow, Russian Federation*

Double calcium/ammonium pyrophosphate monohydrate $Ca(NH_4)_2P_2O_7 \cdot H_2O$ was synthesized as a result of the interaction of calcium carbonate, an aqueous solution containing pyrophosphoric and lactic acids, and ammonia. The synthesized powder turned black after the thermal treatment in a range of 500—700 °C due to amorphous carbon, which is a product of the destruction of the organic nature components present in the prepared powder. After the thermal treatment at 500 °C, the powder is amorphous to X-rays. The phase composition of the powder after the thermal treatment at 600 °C is presented by β-calcium polyphosphate β-$Ca(PO_3)_2$, while β-calcium polyphosphate β-$Ca(PO_3)_2$ and tromelite $Ca_4P_6O_{19}$ are observed after the thermal treatment at 700 °C. The calcium phosphate powder colored due to presence of amorphous carbon can be used as a photocured suspension component that increases the resolution in stereolithographic printing of pre-ceramic semifinished products with a specified geometry of the pore space of calcium phosphate ceramic matrices. The synthesized powder of double calcium/ammonium pyrophosphate monohydrate $Ca(NH_4)_2P_2O_7 \cdot H_2O$ can be applied as a precursor of biocompatible phases for the fabrication of calcium phosphate ceramics used in medicine for the treatment of bone tissue defects.

Key words: ion exchange, pyrophosphoric acid, lactic acid, calcium/ammonium pyrophosphate, amorphous carbon, calcium polyphosphate, tromelite, bioceramics.

Calcium phosphates are of interest for researchers, since they are used as food additives, fertilizers, and pharmaceuticals. The application of materials based on calcium phosphates is due to the chemical composition of the inorganic component of the bone tissue presented by carbonated hydroxyapatite.[1] Bioresorbable materials are necessary to the development of the modern regenerative methods of treatment of bone tissue defects.[2] Advantages of inorganic synthetic bioresorbable materials are the absence of the immune reaction of the organism (unlike that in the case of xenoimplants or allotransplants) and the exclusion of additional traumatic cases compared to the use of autoimplants.[3,4] At the initial stage of treatment, bioresorbable inorganic synthetic materials fill the space of a bone defect and, being porous, provide conditions for the propagation and growth of bone cells and then are gradually dissolved and substituted by the recovered bone tissue. For inorganic materials, bioresorbability is related to such a property as solubility.[5,6]

Tricalcium phosphate ($Ca_3(PO_4)_2$, Ca/P = 1.5), calcium pyrophosphate ($Ca_2P_2O_7$, Ca/P = 1), tromelite ($Ca_4P_6O_{19}$, Ca/P = 0.67), and calcium polyphosphate ($Ca(PO_3)_2$, Ca/P = 0.5)[7] are known among biocompatible and bioresorbable ceramic calcium phosphate materials. According to the literature data, the materials containing these phases are biocompatible and biodegradable.

Sintering additives that make it possible to decrease the annealing temperature due to melt formation are used in order to save energy and thermal equipment service life and to control the process of ceramic microstructure formation.[8] These additives can be inorganic powders of an eutectic composition[9,10] or substances with a low melting temperature,[11,12] the presence of which does not violate the key characteristics of the ceramic material. Of the listed above calcium phosphates, calcium polyphosphate

* Dedicated to Academician of the Russian Academy of Sciences V. V. Lunin on the occasion of his 80th birthday.

Published in Russian in *Izvestiya Akademii Nauk. Seriya Khimicheskaya,* No. 1, pp. 0139—0147, January, 2020.
1066-5285/20/6901-0139

$Ca(PO_3)_2$ with the molar ratio Ca/P = 0.5 is characterized by the lowest melting point (970—1020 °C).[13] Therefore, calcium polyphosphate $Ca(PO_3)_2$ can be considered not only as the biocompatible and bioresorbable phase but also as a component capable of controlling the processes of sintering and formation of the calcium phosphate ceramic material with specified phase composition and microstructure.

Synthetic powders of the substances with a similar Ca/P ratio are used as direct[7] precursors of the $Ca(PO_3)_2$ calcium polyphosphate phase: $Ca(H_2PO_4)_2$, $Ca(H_2PO_4)_2 \cdot H_2O$,[14,15] $CaH_2P_2O_7$,[16] $CaH_2P_2O_7 \cdot H_2O$,[17] $CaNH_4HP_2O_7$,[18,19] $Ca(NH_4)_2P_2O_7 \cdot H_2O$,[20] $Ca_2NH_4H_3(P_2O_7)_2 \cdot H_2O$, $Ca_2NH_4H_3(P_2O_7)_2 \cdot 3H_2O$,[21] $CaH_2(HPO_3)_2$,[22] and $Ca(PO_3) \cdot xH_2O$.[23] Calcium polyphosphate $Ca(PO_3)_2$ with the specified ratio Ca/P = 0.5 is formed due to the thermal transformation of these salts on heating.

Monocalcium phosphate monohydrate $Ca(H_2PO_4)_2 \cdot H_2O$ is applied most frequently as a precursor for the preparation of the calcium polyphosphate[24,25] or the calcium polyphosphate phase in the ceramic material.[26] The formation of double calcium/ammonium phosphates/pyrophosphates as possible products of the reaction of monocalcium phosphate monohydrate $Ca(H_2PO_4)_2H_2O$ and carbamide $CO(NH_2)_2$ has previously been considered predominantly in the works devoted to the production of complex fertilizers[27,28] or during preparation of cements due to the acid—base interaction of ammonium dihydrophosphate $NH_4H_2PO_4$ and calcium aluminates.[29] Double calcium/ammonium orthophosphates were synthesized from calcium oxide CaO, calcium hydroxide $Ca(OH)_2$ or calcium carbonate $CaCO_3$, and monoammonium phosphate $NH_4H_2PO_4$ using mechanical activation.[30] Insignificant amounts of double calcium/ammonium pyrophosphates were found in the products of the interaction of montmorrilonite and calcite with ammonium polyphosphates.[31]

Manufacturing of inorganic materials with specified properties, such as ceramic or cement stone, requires the use of synthetic highly dispersed powders as precursors of certain phase and chemical compositions.[32]

The synthesis of the powders by precipitation from solutions is the stage appropriate for introduction of additional components into the powder composition for the purpose of further use in certain methods for the preparation of ceramic materials with both specified phase composition and specified morphology/architecture/shape. Stereolithographic printing from suspensions containing a photocured monomer and inorganic highly dispersed powder is applied for the preparation of the osteoconductive material.[33] In this case, the lateral resolution of printing can substantially be improved by the introduction of dyes,[34] the most efficient of which is carbon.[35] A component of organic nature can be a source of carbon formed at the stage of preliminary thermal treatment in the calcium phosphate powder. For example, a reaction by-product can serve as this component. The following reaction by-products were used as an amorphous carbon source in synthetic calcium phosphate powders: ammonium formate,[36] ammonium acetate,[23,37] ammonium saccharate,[38] ammonium lactate,[39] and ammonium malate.[40]

The purpose of this work is the preparation and study of powder of double calcium/ammonium pyrophosphate monohydrate $Ca(NH_4)_2P_2O_7 \cdot H_2O$ containing ammonium lactate as a reaction by-product. This powder simultaneously containing the direct precursor of calcium phosphate and the precursor of amorphous carbon will be required as a component of photocured suspensions for stereolithographic printing of porous pre-ceramic semifinished products.

Experimental

The double calcium/ammonium pyrophosphate monohydrate $Ca(NH_4)_2P_2O_7 \cdot H_2O$ powder was synthesized from calcium carbonate $CaCO_3$ (GOST 4530-76) and a solution containing pyrophosphoric $H_4P_2O_7$ and lactic $C_3H_5O_3H$ (Rushim) acids with the addition of an aqueous solution of ammonia $NH_3 \cdot H_2O$ (GOST 3760-79).

Pyrophosphoric acid $H_4P_2O_7$ was prepared using the dynamic ion exchange method.[41] The change in the color of the cation-exchange resin and the shift of the ion exchange front made it possible to visually monitor the ion exchange reaction. A solution of sodium pyrophosphate $Na_4P_2O_7$ (1 L, 0.25 mol L^{-1}) was prepared from $Na_4P_2O_7 \cdot 10H_2O$ (GOST 342-77) and passed (with a rate of 2—3 mL min^{-1}) through a column 5 cm in diameter packed with the KU-2-8 ion-exchange resin preliminarily transformed into the H form (GOST 20298-74). The process occurred can formally be presented by the following reaction equation (1):

$$Na_4P_2O_{7(s)} + 4\ H^+_{(r)} \longrightarrow H_4P_2O_{7(s)} + 4\ Na^+_{(r)}, \qquad (1)$$

where s and r designate the solution and resin, respectively.

Portions of the solution (50 mL each) were collected at the outlet of the column to monitor the quality of the obtained pyrophosphoric acid. The content of Na^+ ions in the portions of acid solutions obtained by dynamic ion exchange was determined by the flame-photometric method on a Flapho 4 two-channel photometer. The analytic signal was obtained by measuring the radiation intensity from atoms of the determined element (Na^+) excited in the flame of a combustible gas mixture (propane—air), and the calibration plot was constructed by standard solutions with the known Na^+ concentrations from $1 \cdot 10^{-4}$ to $1 \cdot 10^{-3}$ g-equiv. L^{-1}. The concentration of pyrophosphoric acid $H_4P_2O_7$ in samples of the solutions was determined by titration with a solution of alkali NaOH (C(NaOH) = 0.1 mol L^{-1}). The sample volume V_p was 1 mL. The acid concentration C_a (in normality units g-equiv. L^{-1}) was calculated by the equation

$$C_a = C(\text{NaOH})V(\text{NaOH})/V_p,$$

where V(NaOH) is the volume of alkali required for the neutralization of the acid in the solution.

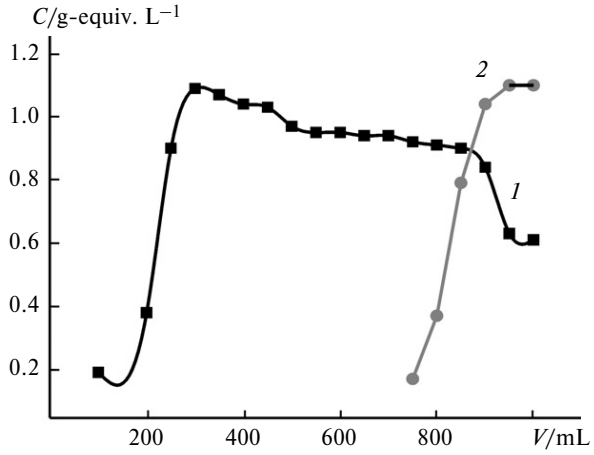

Fig. 1. Dependences of the concentrations of H^+ (*1*) and Na^+ (*2*) on the volume of the solution passed through the column.

The neutralization of the acid with the alkali was monitored by a change in the pH using an Econix-Expert-001 pH meter-ionometer (Russia).

The dependences of the concentrations of Na^+ and H^+ on the volume of the solution passed through the column are presented in Fig. 1.

The portions, in which the Na^+ content did not exceed the lower boundary of concentrations of the calibrated plot, and solutions of the acid with the maximum acid concentration and the absence of Na^+ were used for the synthesis. According to these criteria, ~400 mL of pure pyrophosphoric acid were obtained from 1 L of the initial aqueous solution of sodium pyrophosphate.

A 0.25 *M* solution (100 mL) of lactic acid was added with stirring to a 0.25 *M* solution (100 mL) of pyrophosphoric acid formed due to the dynamic ion exchange. Then calcium carbonate was added in such a way that the ratio Ca/P = 0.5 was fulfilled. This was accompanied by gas evolution, and the formation of water-soluble salts could proceed *via* reactions (2) and (3):

$$2\,C_3H_5O_3H + CaCO_3 \longrightarrow \longrightarrow Ca(C_3H_5O_3)_2 + CO_2 + H_2O, \quad (2)$$

$$H_4P_2O_7 + CaCO_3 \longrightarrow CaH_2P_2O_7 + CO_2 + H_2O. \quad (3)$$

A 25% aqueous solution of ammonia (GOST 3760-79) was added to the obtained transparent solution in order to precipitate double calcium/ammonium pyrophosphate monohydrate. The precipitate was separated from the mother liquor on the Büchner funnel and then dried in thin layer at ~20 °C.

After drying the powder was disaggregated in a planetary mill in an acetone (GOST 2603-79) medium for 15 min using grinding media (balls made from zirconium dioxide) at the ratio powder weight to weight of grinding media equal to 1 : 5. Then the powder was dried at ~20 °C for 2 h in air and passed through a sieve with the cell 200×200 μm. Using the Carver Laboratory Press model manual press (USA), compact powder semifinished products were prepared as pellets 12 mm in diameter and 2—3 mm in height under a pressure of 100 MPa without using a temporary technological binder. The molded powder semifinished products were annealed in a furnace at various temperatures in a range of 500—700 °C (heating rate 5 °C min^{-1}, holding for 2 h at a specified temperature, and cooling together with the furnace).

The linear shrinkage and geometric density of the ceramic samples were determined by measuring their weight and sizes (with an accuracy of ±0.05 mm) before and after annealing.

The X-ray diffraction analyses (XRD) of the synthesized powder and samples after annealing were conducted on a Rigaku D/Max-2500 diffractometer (Japan) with a rotating anode using Cu-Kα radiation. Qualitative phase analysis was carried out using the ICDD PDF2 database.[42]

Simultaneous thermal analysis (STA) was carried out on a NETZSCH STA 409 PC Luxx thermoanalyzer (NETZSCH, Germany) at a heating rate of 10 °C min^{-1}. The weight of the sample was at least 10 mg. The composition of the gas phase formed upon sample decomposition was studied on a QMS 403C Aëolos quadrupole mass spectrometer (NETZSCH, Germany) combined with a NETZSCH STA 409 PC Luxx thermoanalyzer. Ionization was performed with a beam of fast electrons with the ionization energy 70 eV. Mass spectra were recorded for the following mass numbers *m/z*: 18 $[H_2O]^+$, 44 $[CO_2]^+$, 15 $[NH]^+$, and 30 $[NO]^+$.

The microstructures of the samples were studied by scanning electron microscopy (SEM) on a LEO SUPRA 50VP electron microscope (Carl Zeiss, Germany; autoemission source) at an accelerating voltage of 3—20 kV in secondary electrons using an SE2 detector. A chromium layer (up to 10 nm) was sputtered on the sample surface.

Results and Discussion

According to the XRD data (Fig. 2), we synthesized the powder of double calcium/ammonium pyrophosphate monohydrate $Ca(NH_4)_2P_2O_7 \cdot H_2O$ (PDF 44-754 card).

The precipitate $Ca(NH_4)_2P_2O_7 \cdot H_2O$ was formed *via* reaction (4):

$$CaH_2P_2O_7 + 2\,NH_3 \cdot H_2O \longrightarrow \longrightarrow Ca(NH_4)_2P_2O_7 \cdot H_2O + H_2O. \quad (4)$$

Since an aqueous solution of ammonia was added until pH 9 was achieved in the reaction zone, then water-soluble ammonium lactate was also formed according to reaction (5):

$$2\,C_3H_5O_3H + 2\,NH_3 \cdot H_2O \longrightarrow C_3H_5O_3NH_4 + H_2O. \quad (5)$$

Ammonium lactate present in the mother liquor was adsorbed on the surface of synthesized particles of the powder of double calcium/ammonium pyrophosphate monohydrate $Ca(NH_4)_2P_2O_7 \cdot H_2O$. The amount of dissolved substances adsorbed from the mother liquor on the surface of the synthesized particles depends substantially on their concentration in the solution. For example, the concentration of the soluble by-product of the synthesis of calcium phosphates depends on the concentration of solutions of the initial reagents.[43] It is most likely that a low concentration of the initial solutions, a lower surface area of the specific surface of particles of calcium phos-

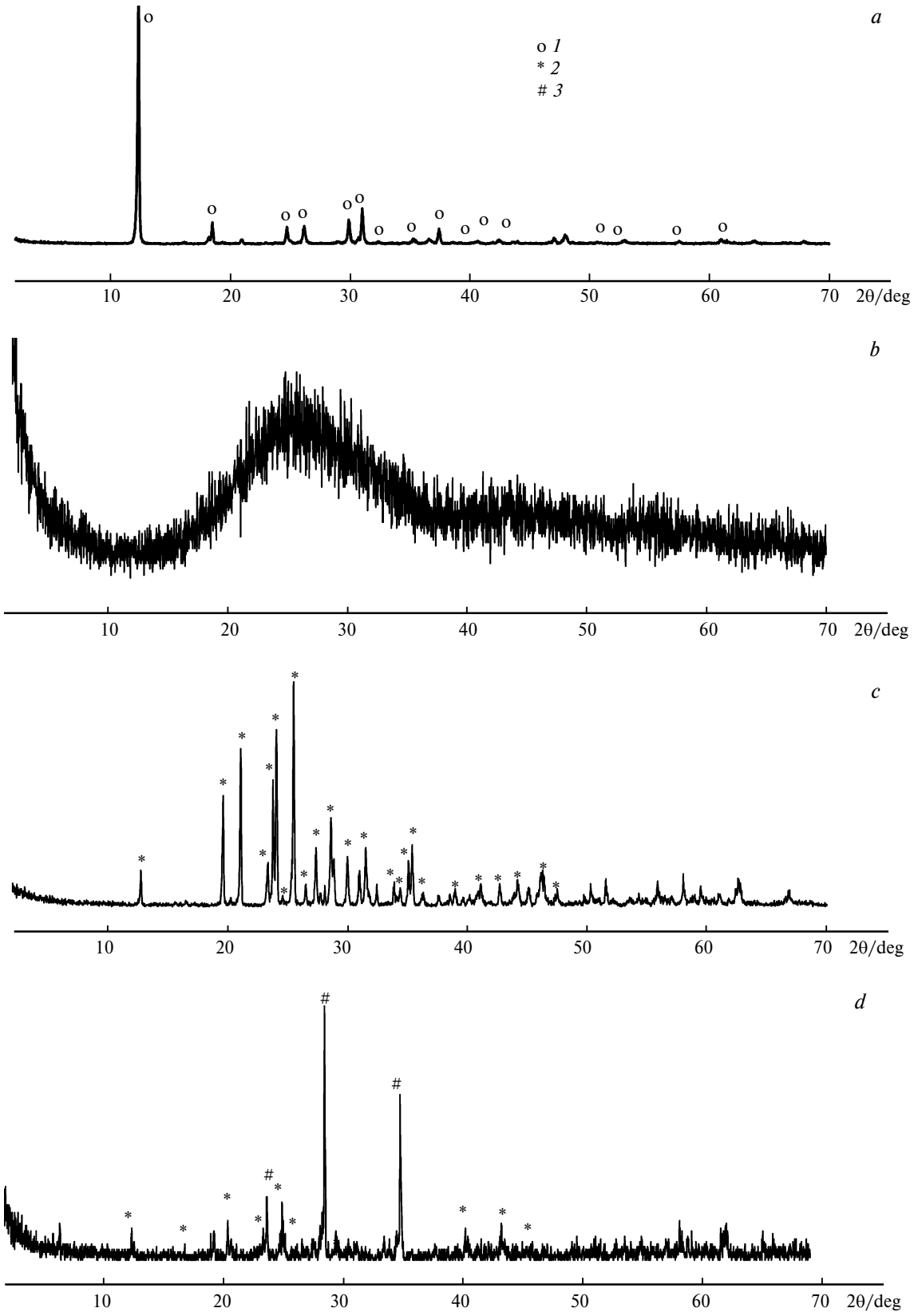

Fig. 2. XRD data for the powder after the synthesis (*a*) and thermal treatment at 500 (*b*), 600 (*c*), and 700 °C (*d*): *1*, $Ca(NH_4)_2P_2O_7 \cdot H_2O$ (PDF 44-754 card); *2*, β-$Ca(PO_3)_2$ (PDF 11-39 card); and *3*, $Ca_4P_6O_{19}$ (PDF 18-177 card).

phates of lamellar morphology (for example, brushite)[44] compared to the specific surface area of the surface of the particles with the shape close to isometric (*e.g.*, hydroxyapatite)[43] during the synthesis from solutions of the same salts with the same concentration, and a restricted sensitivity of the XRD method did not allow us to determine the presence of ammonium lactate or lactic acid.

The powder was aggregated, and the aggregate size was 8—30 μm (Fig. 3, *a*). The powder particles were characterized by the lamellar morphology and were 300—2000 nm in size with a thickness of ~50 nm (Fig. 3, *b*).

According to the STA data, the total mass loss on heating to 1000 °C was 28% (Fig. 4).

According to the results of studying by mass spectrometry, several temperature ranges where water is isolated can be distinguished in the curve for $m/z = 18$ (Fig. 5). An insignificant amount of physically bound water is isolated in a range of 40—140 °C. The next bright peak, which reflects, most likely, hydrate water isolation from $Ca(NH_4)_2P_2O_7 \cdot H_2O$ (reaction (6)), is in a range of 180—270 °C.

$$Ca(NH_4)_2P_2O_7 \cdot H_2O \longrightarrow H_2O + Ca(NH_4)_2P_2O_7 \quad (6)$$

Water formation in the range 400—600 °C (slope low-intensity peak) is probably related to the decomposition of residues of the organic component.

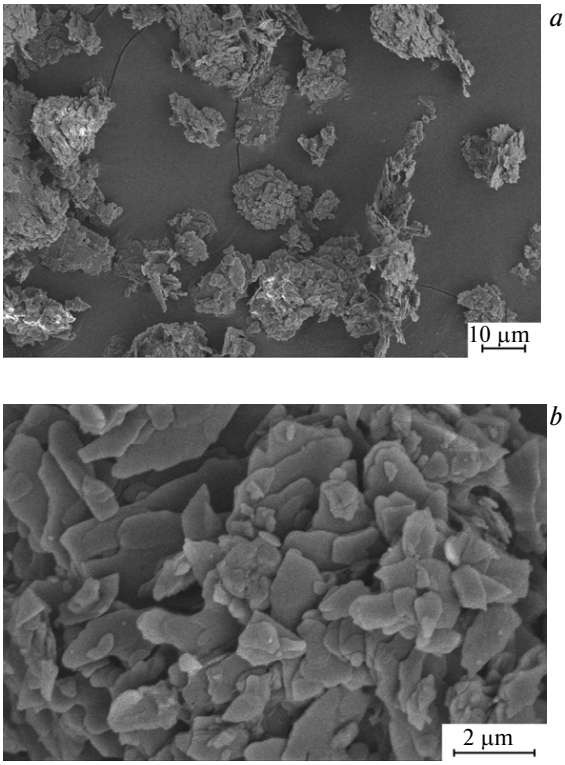

Fig. 3. SEM images of the powder after the synthesis: amplification ×2000 (*a*) and ×20000 (*b*).

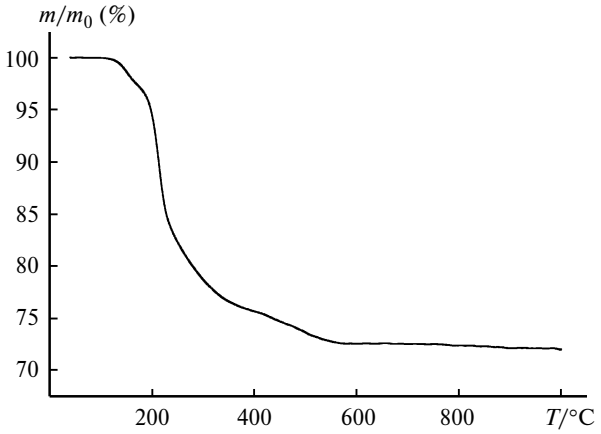

Fig. 4. STA data: temperature dependence of the mass loss.

Two distinct peaks are observed on the curve for $m/z = 15$ (the formation of $[NH]^+$ repeats the formation of $[NH_3]^+$). According to the data of mass spectrometry, the concerted isolation of carbon dioxide ($m/z = 44$) and ammonia ($m/z = 15$), occurs in a range of 120—210 °C, which can be caused by the decomposition of ammonium lactate (reaction (7)).

$$C_3H_5O_3NH_4 + 3\,O_2 \longrightarrow 3\,CO_2 + 3\,H_2O + NH_3 \quad (7)$$

However, as shown by an experience of the authors[36—39] and the practice of conducting a number of catalytic processes,[45] organic substances adsorbed on the surface of the inorganic oxide materials are often subjected to carbonization on heating, most likely, due to oxygen deficiency or for kinetic reasons. The black color of the powders after the thermal treatment in a range of 500—700 °C confirms the possibility for this process to occur, which can be presented by reactions (8) and/or (9).

$$C_3H_5O_3NH_4 + 2\,O_2 \longrightarrow C + 2\,CO_2 + 3\,H_2O + NH_3, \quad (8)$$

$$C_3H_5O_3NH_4 + O_2 \longrightarrow 2\,C + CO_2 + 3\,H_2O + NH_3. \quad (9)$$

The formation of dilactides, oligomers of polylactic acid, or polylactides and their subsequent thermal destruction cannot be excluded on heating of ammonium lactate.[46,47]

The second peak on the curve for $m/z = 15$ in a range of 200—350 °C, which is overlapped with the main range of water formation (180—270 °C), is probably related to the transformation of double calcium/ammonium pyrophosphate $Ca(NH_4)_2P_2O_7$ into calcium polyphosphate $Ca(PO_3)_2$ (reaction (10)).

$$Ca(NH_4)_2P_2O_7 \longrightarrow H_2O + 2\,NH_3 + Ca(PO_3)_2 \quad (10)$$

Ammonia isolated on heating in air can be oxidized to form nitrogen oxides. The formation of nitrogen oxides

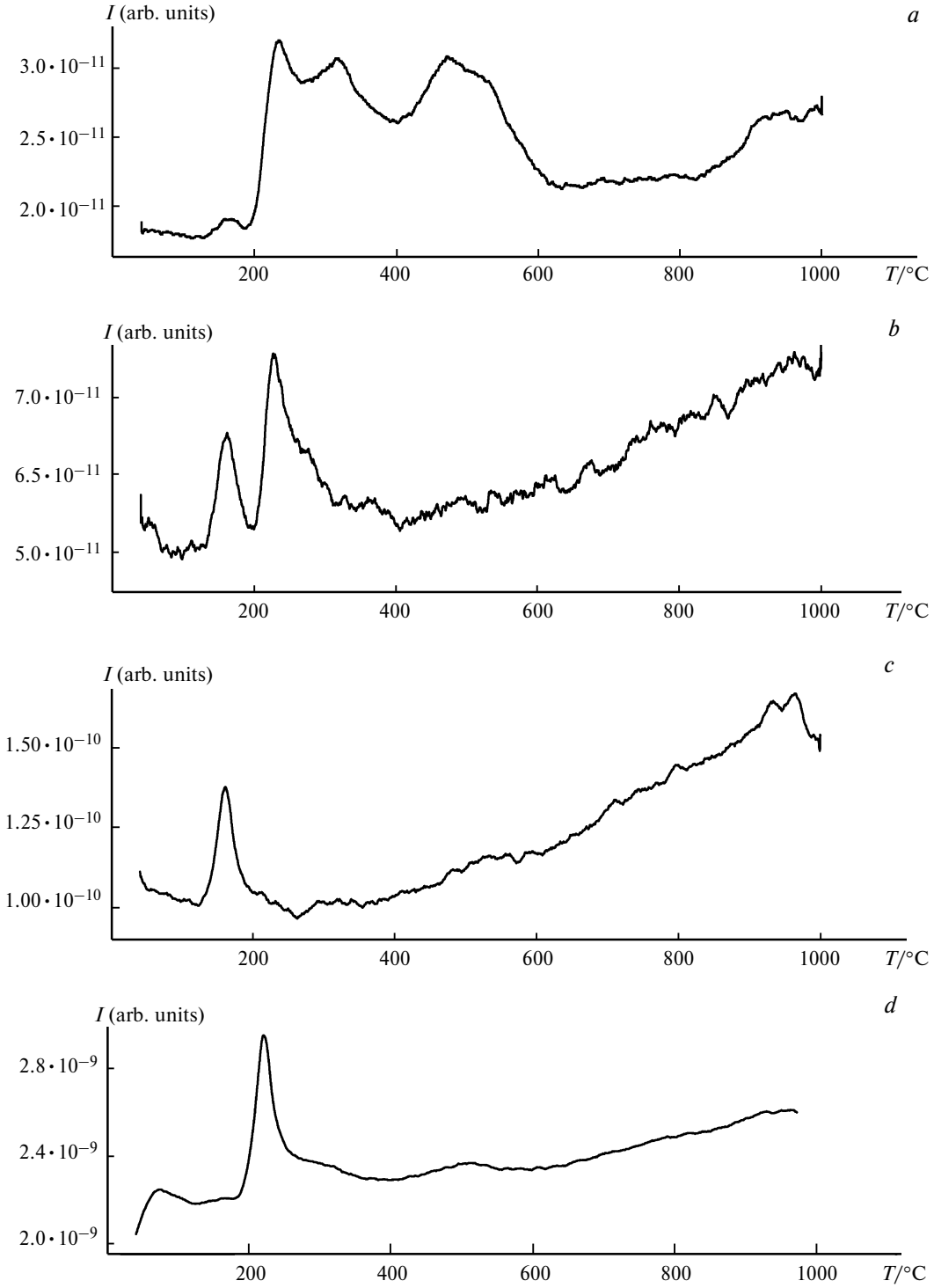

Fig. 5. Mass spectrometric curves for $m/z = 30$ $[NO]^+$ (*a*), 15 $[NH]^+$ (*b*), 44 $[CO_2]^+$ (*c*), and 18 $[H_2O]^+$ (*d*).

is illustrated for $[NO]^+$ ($m/z = 30$) as an example. The peaks on the curve for $m/z = 30$ accompany the above described peaks for $m/z = 15$. In addition, several peaks in ranges of 270—400 and 400—620 °C can be distinguished on the curve for $[NO]^+$ ($m/z = 30$). It is most likely that these peaks can be assigned to the transformation of double calcium/ammonium pyrophosphate $Ca(NH_4)_2P_2O_7$ into calcium polyphosphate $Ca(PO_3)_2$ continued on heating.

The shape of the curve for $m/z = 44$ assumes that CO_2 isolated at the temperature >300 °C due to the gradual

oxidation of the earlier formed products of destruction of organic components and carbon.

The XRD data indicate that the powder is amorphous to X-rays after the thermal treatment at 500 °C (see Fig. 2). Only after the thermal treatment at 600 °C, the powder is transformed into β-calcium polyphosphate β-$Ca(PO_3)_2$. An increase in the thermal treatment temperature to 700 °C results in the formation of the two-phase material containing both β-calcium polyphosphate β-$Ca(PO_3)_2$ and tromelite $Ca_4P_6O_{19}$ (reaction (11)).

$$4\ Ca(PO_3)_2 + H_2O = Ca_4P_6O_{19} + 2\ HPO_3 \qquad (11)$$

A similar phenomenon was also observed when studying[23] the thermal evolution of calcium polyphosphate $Ca(PO_3)_2$ obtained from hydrated polyphosphate $Ca(PO_3)_2 \bullet xH_2O$. Thus, the synthesized powder can be considered as a single-phase precursor for the synthesis of a composite ceramic material. The use of the single-phase powder precursor allows one to prepare multiphase ceramics with a high uniformity of the phase distribution.[23,48]

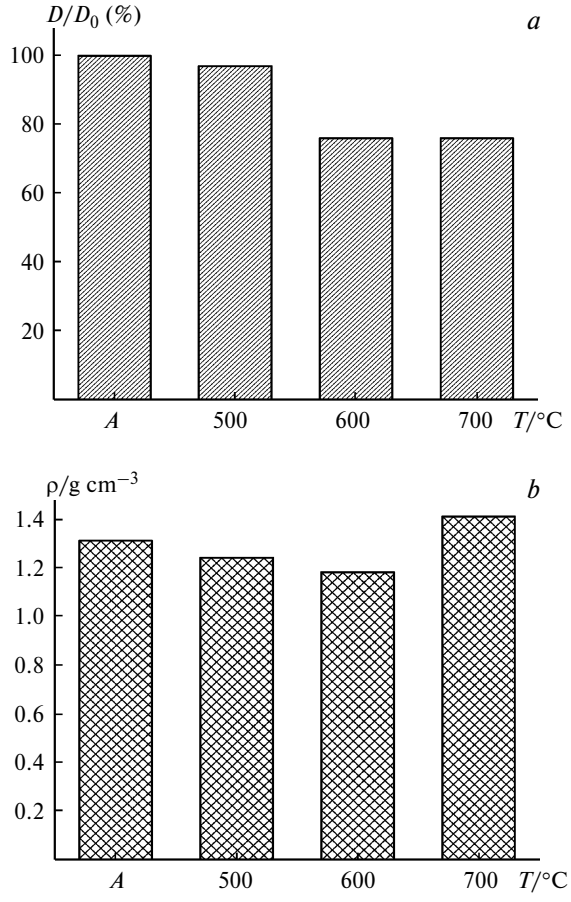

Fig. 6. Dependences of the diameter (*a*) and density (*b*) of the samples pressed from the synthesized powder on the thermal treatment temperature; *A*, after pressing.

The linear shrinkage after the thermal treatment at 700 °C for the powdered compact samples prepared by pressing under a pressure of 100 MPa was 24% (Fig. 6, *a*). The geometric density (Fig. 6, *b*) after pressing was 1.3 g cm^{-3}. Then the density decreased because of the decomposition processes that occurred and the absence of sintering at 500 and 600 °C, while after the thermal treatment at 700 °C the geometric density somewhat exceeded the initial density of the pressed sample being 1.4 g cm^{-3}.

The micrographs of the cuts of the samples after annealing at 500 and 700 °C are presented in Fig. 7.

After annealing at 500 °C, the lamellar morphology and size of the initial particles in the sample are predominantly retained (see Fig. 7, *a*). The regions on which local sintering took place are observed. After annealing at 700 °C, the obtained ceramic material was characterized by heterogeneous porosity with the pore size from 200 nm to 4—8 μm (see Fig. 7, *b*). It seems impossible to isolate the grain boundaries or determine the grain size in the material. In this study, we present the data of test annealings of the compact samples from the powder that can be used as a sintering additive decreasing the annealing temperature or as an additional component of ceramic suspensions for stereolithographic printing. In order to attain the expected effect (a decrease in the annealing temperature

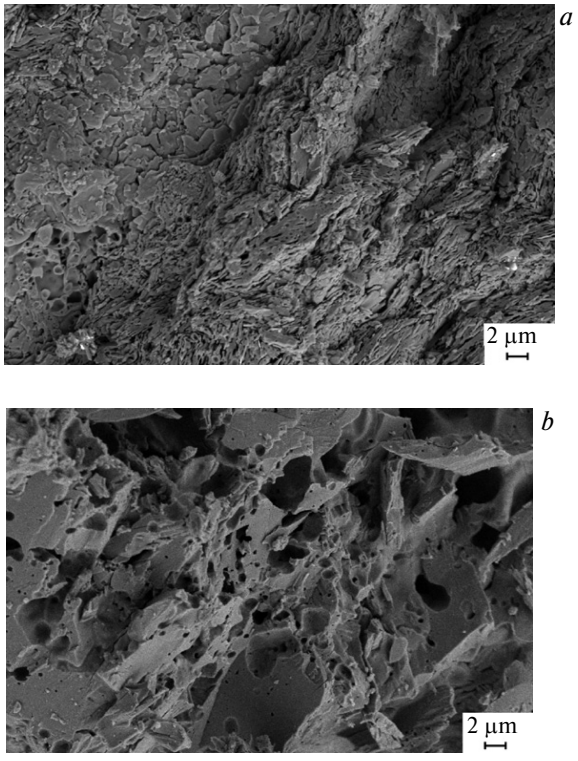

Fig. 7. SEM images of the cuts of the ceramic samples after the thermal treatment at 500 (*a*) and 700 °C (*b*) for 2 h.

or an increase in the lateral resolution of stereolithographic printing), the synthesized powder of double calcium/ammonium pyrophosphate monohydrate $Ca(NH_4)_2P_2O_7 \cdot H_2O$ or the colored powder of calcium polyphosphate $Ca(PO_3)_2$ should uniformly be distributed in a powdered mixture of calcium phosphates with a higher Ca/P molar ratio or in a suspension for molding. To conclude, double calcium/ammonium pyrophosphate monohydrate $Ca(NH_4)_2P_2O_7 \cdot H_2O$ was synthesized for the first time by precipitation from the solution containing Ca^{2+} ions, pyrophosphoric and lactic acids, and an aqueous solution of ammonia. The biocompatible phases are formed due to the thermal conversion during the thermal treatment of $Ca(NH_4)_2P_2O_7 \cdot H_2O$: the first formed β-calcium polyphosphate β-$Ca(PO_3)_2$ (600 °C) is then transformed into the two-phase material containing β-calcium polyphosphate β-$Ca(PO_3)_2$ and tromelite $Ca_4P_6O_{19}$ (700 °C). The presence of ammonium lactate $C_3H_5O_3NH_4$ in the synthesized powder makes it possible to impart a black color to the powder of β-calcium polyphosphate β-$Ca(PO_3)_2$ or the powder containing β-calcium polyphosphate β-$Ca(PO_3)_2$ and tromelite $Ca_4P_6O_{19}$ due to the thermal treatment. The black-colored calcium phosphate powder can be applied as a component of the suspension increasing the lateral resolution during molding of units by stereolithographic 3D printing. The obtained powder of double calcium/ammonium pyrophosphate monohydrate $Ca(NH_4)_2P_2O_7 \cdot H_2O$ can be used for the preparation of ceramic biocompatible and bioresorbable calcium phosphate materials as the precursor of the phase of calcium polyphosphate $Ca(PO_3)_2$ with a lowered melting point (970—1020 °C), which can act as a sintering additive decreasing the sintering temperature.

The study was carried out using the equipment purchased in the framework of the Program of Development of the Moscow State University.

This work was financially supported by the Russian Foundation for Basic Research (Project No. 18-29-11079).

References

1. S. M. Danil´chenko, S. N. Danil´chenko, *Visnik SumDU. Ser. Fizika, Matematika, Mekhanika* [*Bull. Sumy Univ. Ser. Math., Phys. Mech.*], 2007, No. 2, 33 (in Russian); http://essuir.sumdu.edu.ua/bitstream/123456789/1152/1/3_Danil.pdf.
2. S. Pina, V. P. Ribeiro, C. F. Marques, F. R. Maia, T. H. Silva, R. L. Reis, J. M. Oliveira, *Materials*, 2019, **12**, 1824.
3. V. N. Mudraya, I. G. Stepanenko, A. S. Shapovalov, *Ukr. Zh. Klinich. Labor. Medyts.* [*Ukr. J. Clin. Labor. Medic.*], 2010, **5**, No. 1, 52 (in Russian).
4. S. Titsinides, G. Agrogiannis, T. Karatzas, *Jpn Dent. Sci. Rev.*, 2019, **55**, No. 1, 26.
5. P. D. Sarkisov, N. Y. Mikhailenko, E. E. Stroganova, N. V. Buchilin, S. P. Baskov, *Glass Ceram.*, 2012, **69**, No. 5—6, 173.
6. J. Jeong, J. H. Kim, J. H. Shim, N. S. Hwang, C. Y. Heo, *Biomater. Res.*, 2019, **23**, 1, 4.
7. T. V. Safronova, V. I. Putlyaev, *Inorg. Mater.*, 2017, **53**, 17.
8. A. P. Savitskii, *Zhidkofaznoe spekanie sistem s vzaimodeistvuyushchimi komponentami* [*Liquid-Phase Sintering of Systems with Interacting Components*], Nauka, Novosibirsk, 1991, 184 pp. (in Russian).
9. N. A. Makarov, *Glass Ceram.*, 2006, **63**, No. 3—4, 119.
10. M. N. Safina, T. V. Safronova, E. S. Lukin, *Glass Ceram.*, 2007, **64**, No. 7—8, 238.
11. W. Suchanek, M. Yashima, M. Kakihana, M. Yoshimura, *Biomaterials*, 1997, **18**, 923.
12. T. F. Safronova, V. I. Putlyaev, Ya. Yu. Filippov, D. S. Larionov, P. V. Evdokimov, A. E. Averina, E. S. Klimashina, V. K. Ivanov, *Refract. Ind. Ceram.*, 2015, **56**, No. 1, 43.
13. M. Weil, M. Puchberger, J. Schmedt auf der Guenne, J. Weber, *Chem. Mater.*, 2007, **19**, 5067.
14. G. MacLennan, C. A. Beevers, *Acta Crystallogr.*, 1956, **9**, 187.
15. B. Boonchom, C. Danvirutai, *J. Optoelectron. Biomed. Mater.*, 2009, No. 1, 115.
16. L. E. Jackson, A. J. Wright, *Key Eng. Mater.*, 2005, **284**, 71.
17. J. Trommer, M. Schneider, H. Worzala, A. N. Fitch, *Mater. Sci. Forum*, 2000, **321**, 374.
18. E. H. Brown, W. E. Brown, J. R. Lehr, J. P. Smith, A. W. Frazier, *J. Phys. Chem.*, 1958, **62**, 366.
19. L. R. Hossner, J. R. Melton, *Soil Sci. Soc. Am. J.*, 1970, **34**, 801.
20. Y. V. Subbarao, R. Ellis, *Soil Sci. Soc. Am. J.*, 1975, **39**, 1085.
21. E. H. Brown, J. R. Lehr, J. P. Smith, A. W. Frazier, *J. Agr. Food Chem.*, 1963, **11**, 214.
22. D. Zobel, N. Ba, *Z. Chem.*, 1969, **9**, 433.
23. T. V. Safronova, E. A. Mukhin, V. I. Putlyaev, A. V. Knotko, P. V. Evdokimov, T. B. Shatalova, Ya. Yu. Filippov, A. V. Sidorov, E. A. Karpushkin, *Ceram. Int.*, 2017, **43**, No. 1, 1310.
24. P. Prokupkova, P. Mošner, L. Koudelka, M. Vlček, *J. Mater. Sci.*, 1998, **33**, 743.
25. L. E. Jackson, B. M. Kariuki, M. E. Smith, J. E. Barralet, A. J. Wright, *Chem. Mater.*, 2005, **17**, 4642.
26. T. V. Safronova, V. I. Putlyaev, A. V. Knot'ko, V. K. Krut´ko, O. N. Musskaya, S. A. Ulasevich, N. A. Vorob´eva, V. D. Telitsin, *Glass and Ceram.*, 2018, **75**, No. 7—8, 279.
27. O. B. Dormeshkin, N. I. Vorob´ev, G. Kh. Cherches, A. N. Gavrilyuk, *Trudy BGTU. Khim. Tekhn. Neorg. Veshchestv* [*Workds of BGTU. Chem. Techn. Inorg. Substances*], 2008, **1**, No. 3, 65 (in Russian).
28. O. Dormeshkin, *Interactions Between Components of Complex Fertilizers. Chemical and Physico-Chemical Interactions at the Stages of Mixing, Granulating and Drying During their Production*, Lap Lambert Academic Publishing, Mauritius, 2019, 57 pp.
29. T. Sugama, M. Allan, J. M. Hill, *J. Am. Ceram. Soc.*, 1992, **75**, 8, 2076.
30. L. Sharma, D. Kiani, K. Honer, J. Baltrusaitis, *ACS Sustainable Chem. Eng.*, 2019, **7**, 6802.
31. O. D. Philen, J. R. Lehr, *Soil Sci. Soc. Am. J.*, 1967, **31**, 196.
32. N. T. Andrianov, V. L. Balkevich, A. V. Belyakov, A. S. Vlasov, I. Ya. Guzman, E. S. Lukin, Yu. M. Mosin, B. S. Skidan, *Khimicheskaya tekhnologiya keramiki: ucheb. posobie dlya vuzov* [*Chemical Technology of Ceramics: Manual for Higher Educational Institutions*], Ed. I. Ya. Guzman, OOO Rif Stroimaterialy, Moscow, 2012, 496 pp. (in Russian).

33. J. W. Halloran, *Annu. Rev. Mater. Res.*, 2016, **46**, 19.
34. Y. Li, M. Wang, H. Wu, F. He, Y. Chen, S. Wu, *J. Eur. Ceram. Soc.*, 2019, **39**, 4921; https://doi.org/10.1016/j.jeurceramsoc.2019.07.035.
35. P. V. Evdokimov, Author´s Abstract, Cand. Sci. (Chem.) Thesis, M. V. Lomonosov Moscow State University, Moscow, 2014, 18 pp. (in Russian).
36. T. V. Safronova, V. I. Putlyaev, Y. Y. Filippov, S. A. Vladimirova, D. M. Zuev, G. S. Cherkasova, *Glass Ceram.*, 2017, **74**, No. 5—6, 185.
37. T. V. Safronova, S. A. Kurbatova, T. B. Shatalova, A. V. Knotko, P. V. Yevdokimov, V. I. Putlyayev, *Inorg. Mater. Appl. Res.*, 2017, **8**, No. 1, 118.
38. T. V. Safronova, G. K. Kazakova, P. V. Yevdokimov, T. B. Shatalova, A. V. Knotko, A. V. Korotkova, V. I. Putlyayev, *Inorg. Mater. Appl. Res.*, 2016, **7**, No. 4, 635.
39. T. V. Safronova, V. I. Putlyaev, M. D. Andreev, Ya. Yu. Filippov, A. V. Knot´ko, T. B. Shatalova, P. V. Evdokimov, *Inorg. Mater.*, 2017, **53**, 859.
40. T. V. Safronova, V. I. Putlyaev, A. V. Knot'ko, T. B. Shatalova, V. Yu. Savinova, *Inorg. Mater. Appl. Res.*, 2019, **10**, 841.
41. A. I. Vulikh, *Ionoobmennyi sintez* [*Ion-Exchange Synthesis*], Khimiya, Moscow, 1973, 232 pp. (in Russian).
42. *ICDD (2010). PDF-4+ 2010* (*Database*), Ed. S. Kabekkodu, International Centre for Diffraction Data, Newtown Square, PA, USA; available online: http://www.icdd.com/products/pdf2.htm (accessed on 12 August 2019).
43. T. V. Safronova, M. A. Shekhirev, V. I. Putlyaev, Y. D. Tret´yakov, *Inorg. Mater.*, 2007, **43**, 901.
44. T. V. Safronova, A. V. Kuznetsov, S. A. Korneychuk, V. I. Putlyaev, M. A. Shekhirev, *Cent. Eur. J. Chem.*, 2009, **7**, 184.
45. V. B. Ioffer, *Osnovy proizvodstva vodoroda* [*Foundations of Hydrogen Production*], Gos. Nauchno-Tekhn. Gorno-Topl. Lit., Leningrad, 1960, 430 pp. (in Russian).
46. I. C. McNeill, H. A. Leiper, *Polym. Degrad. Stab.*, 1985, **11**, 267.
47. I. C. McNeill, H. A. Leiper, *Polym. Degrad. Stab.*, 1985, **11**, 309.
48. E. V. Kukueva, V. I. Putlyaev, A. A. Tikhonov, T. V. Safronova, *Inorg. Mater.*, 2017, **53**, 212.

Received August 27, 2019;
in revised form October 17, 2019;
accepted November 11, 2019